Cloud seeding as a technique for studying aerosol-cloud interactions in marine stratocumulus

Virendra P. Ghate,[1] Bruce A. Albrecht,[1] Pavlos Kollias,[2] Haflidi H. Jonsson,[3] and Daniel W. Breed[4]

Received 19 February 2007; revised 21 May 2007; accepted 20 June 2007; published 19 July 2007.

[1] Giant hygroscopic aerosols were introduced into a solid marine stratocumulus cloud (200 m thick) by burning hygroscopic flares mounted on an aircraft. The cloud microphysical response in two parallel seeding plumes was observed using an instrumented aircraft making 16 transects of the plumes. The cloud drop size distribution width increased in the plumes due to an increased number of small cloud drops (3–5 μm) on the earlier transects and a 5-fold increase in the number of large drops (20–40 μm) relative to the background cloud 30 minutes later. The cloud effective diameter increased from about 11 μm in the background to 13 μm in the plumes. Although the giant nuclei were only a small fraction of the total aerosols produced by the flares, they dominated the cloud response. The merit of the seeding approach for controlled observational studies of aerosol-cloud interactions in marine stratocumulus was demonstrated. **Citation:** Ghate, V. P., B. A. Albrecht, P. Kollias, H. H. Jonsson, and D. W. Breed (2007), Cloud seeding as a technique for studying aerosol-cloud interactions in marine stratocumulus, *Geophys. Res. Lett.*, *34*, L14807, doi:10.1029/2007GL029748.

1. Introduction

[2] Aerosol-cloud interactions in marine stratocumulus may have a strong influence on the albedo [*Twomey*, 1977] and the macroscopic properties [*Albrecht*, 1989] of the clouds. Aircraft *in situ* and remote sensing observations have been used to study these effects due to natural causes [e.g., *Stevens et al.*, 2005; *Sharon et al.*, 2006] and anthropogenic forcing [e.g., *Durkee et al.*, 2000]. In addition, Large Eddy Simulation (LES) that included explicit treatments of aerosol size distributions and cloud microphysics have been applied to marine stratocumulus to study the effects that changes in background Cloud Condensation Nuclei (CCN) have on cloud and drizzle characteristics [e.g., *Feingold et al.*, 1999; *Ackerman et al.*, 2003; *Jiang et al.*, 2002]. Although substantial efforts have focused on understanding how increases in aerosols may increase cloud albedo by decreasing the effective diameter of cloud droplets and cloud lifetime in marine stratocumulus through a reduction of drizzle, it is equally important to understand how increases in aerosols of the right composition and size can increase precipitation efficiency [*Feingold et al.*, 1999].

[3] The shortcomings of observational studies of aerosol-cloud interactions include opportunistic sampling that provides only a narrow window of conditions and limited possibilities to perform controlled experiments. In modeling studies, however, the CCN size distribution can be perturbed in a controlled way and the cloud response can be simulated. *Feingold et al.* [1999], for example, simulated the response of stratocumulus clouds to changes in the concentration of ultragiant nuclei and the resulting effects on drizzle rates and the dependence of these rates on background conditions using LES. But observations confirming these simulations are limited. Ship-tracks observed in marine stratocumulus provide a unique cloud features for studying how increases in aerosols affect cloud properties [e.g., *Durkee et al.*, 2000]. But *in situ* observations of these features require opportunistic sampling and provide limited insight into the time evolution of the cloud response to an uncontrolled aerosol perturbation.

[4] To overcome the shortcomings of passive observations of aerosol-cloud interactions in marine stratocumulus, we explored an active approach–artificial cloud seeding. This approach demonstrates the feasibility of performing controlled experiments in the natural laboratory provided by marine stratocumulus clouds. For the experiment we consider how the artificial introduction of giant hygroscopic nuclei affects cloud physical properties in marine stratocumulus. We use a hygroscopic seeding technique developed for the purpose of stimulating "warm-rain" precipitation production in cumulus clouds [*Mather et al.*, 1997].

2. Instrumentation and Methodology

[5] Our observational strategy was to intentionally perturb the background aerosol field in a solid marine stratocumulus cloud and then to observe the cloud microphysical response to this aerosol perturbation using an instrumented aircraft. The artificial source of aerosols used in this study was flares developed by Ice Crystal Engineering (ICE). They are designed to produce hygroscopic particles with their primary components consisting of Potassium Perchlorate ($KClO_4$) and Calcium Chloride ($CaCl_2$). The burning of these flares produce KCl and $Ca(Cl)_2$ particles that lead to the formation of giant aerosols in the range of 1–5 μm in the form of salt aggregates. The effects that flares of this type have on precipitation formation in cumulus clouds were evaluated using a cloud model by *Cooper et al.* [1997]. For our experiment the Weather Modification Inc.

[1] Division of Meteorology and Physical Oceanography, Rosenstiel School of Marine and Atmospheric Science, University of Miami, Miami, Florida, USA.
[2] Department of Atmospheric and Oceanic Sciences, McGill University, Montreal, Quebec, Canada.
[3] Center for Interdisciplinary and Remotely Piloted Aircraft Studies, Marina, California, USA.
[4] Applied Science Group, Research Application Laboratory, National Center for Atmospheric Research, Boulder, Colorado, USA.

0094-8276/07/2007GL029748

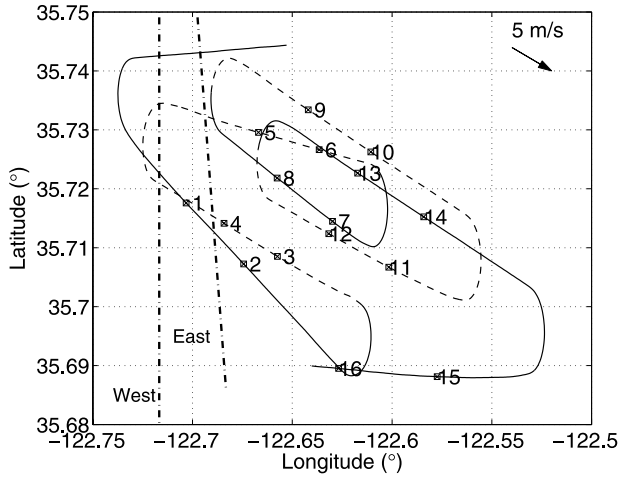

Figure 1. Flight track of the Twin Otter during the seeding experiment on 28 June 2006. The flight level was at 350 m. Numbers correspond to plume crossings. The two dashed-dotted lines indicate the initial flare burn lines conducted by the Cheyenne II aircraft. The dotted and solid lines within the flight track are for clarity purpose only.

(WMI) Cheyenne II aircraft was used for burning ICE flares in the clouds.

[6] The aerosol and cloud microphysical observations were made from the Center for Interdisciplinary Remotely Piloted Aircraft Studies (CIRPAS)'s Twin Otter research aircraft. Instruments on the Twin Otter included three *in-situ* instruments for characterizing aerosol, cloud, and precipitation size distributions - a Passive Cavity Aerosol Spectrometer Probe (PCASP), a Forward Scattering Spectrometer Probe (FSSP) and Cloud Imaging Probe (CIP) that resolve particles in diameter ranges from 0.1–3 μm, 2.25–40 μm and 25–1500 μm respectively. Since counting artifacts were observed in the last bin of PCASP, the first two bins of FSSP and the first bin of CIP, these bins were not used, resulting in no overlap between the instruments. Standard instrumentation was also available to sample the thermodynamic variables and winds.

3. Observations

[7] Real-time visible and IR satellite images were used to identify homogeneous stratus cloud decks. The cloud deck selected for cloud seeding was observed on 28 June 2006 where solid clouds were observed off the coast of central California at ~35.7 N 122.5 W. A low-level sounding in the area of interest was made before seeding to provide boundary layer and cloud properties critical to the design of the seeding flight and post-seeding sampling of the cloud layer. The boundary layer was capped by an inversion at ~450 m, cloud base height was ~250 m, and winds were at 5 ms^{-1} from west-north-west. The mean cloud droplet concentration was about 220 cm^{-3} and no drizzle was observed.

[8] After the initial sounding, the Cheyenne II seeded the clouds along two lines approximately 10 km in length and separated by about 5 km. On each leg 6 ICE flares were burned at the midlevel of the cloud (350 m). Since the mean wind direction was west-north-westerly, the flares were burned in a nearly north-south direction (Figure 1). The Twin Otter started sampling in the cloud about 10 minutes after the seeding was completed. During the in-cloud sampling 16 successful transects were made across the two plumes. The track of the aircraft and the plume crossings are shown in Figure 1. The aircraft made several east-west passes to maximize plume intersects as the seeded lines advected with the mean wind.

[9] Plume intersects with the Twin Otter were easily identified by a pronounced double-peaked increase in the PCASP aerosol concentrations compared with the background cloud values (Figure 2). The onboard real-time display of the PCASP was used to identify the plume crossings and to direct the aircraft for future intersections. For the analysis, the plume intersects were determined objectively using a threshold of 250 cm^{-3} for the PCASP concentrations compared with a background concentration of ~80 cm^{-3}. The intersects were numbered from 1 to 16 and the background areas were labeled from A to I (Figure 2). Observations were made until the on-board PCASP signatures of the plumes were no longer detected.

4. Analysis

[10] The flare aerosol size distribution (Figure 3, top) was obtained by flying through a flare plume generated in clear air above the boundary layer (RH 40%) on a separate day from the main seeding event. Cloud responses to the seeding are seen in some of the spectra starting as early as the first few crossing (t ~ 2 min) as shown in Figure 3 (top), where east plume crossings 2 and 15 are shown along with the flare size distribution and average aerosol and cloud size distributions for background areas sampled. Although the events defined by the PCASP peaks are only few seconds in duration, the spectra clearly show the small particle signatures compared with the background. On intersect 2, increases above the background for particles

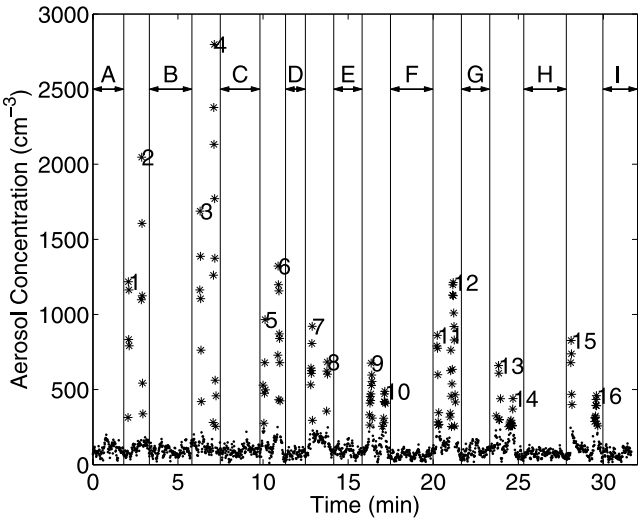

Figure 2. PCASP recorded aerosol concentrations during seeding experiment. Numbers indicate plume crossings (see Figure 1) and vertical lines indicate the boundaries of the plumes. Background areas are designated by letters and were defined for areas outside of the two plumes. Asterisks indicate the plume values which were determined objectively using threshold of 250 cm^{-3}.

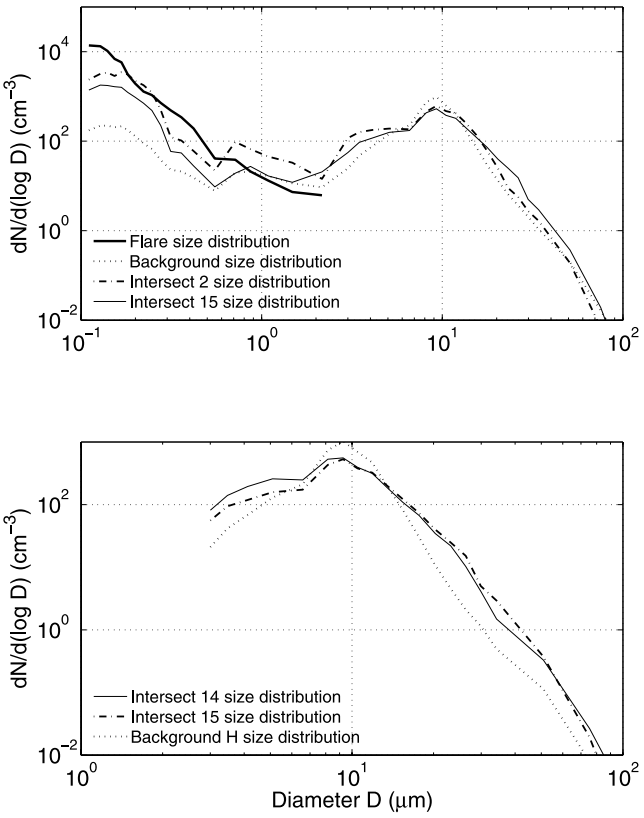

Figure 3. (top) Aerosols and cloud spectra for east plume intersects 2 and 15 with background cloud. The flare size distribution (thick solid line) was obtained from a burn made above the cloud on a separate day. (bottom) Cloud droplet spectra for intersects 14 and 15 with the in-between background H.

in the range of 2–8 μm are clearly observed in addition to the peak increases at 0.1–0.2 μm. The peak at 0.1–0.2 μm is observed in all the crossings, and allows for easy plume identification. For intersect 15 (t $\sim$ 27 min) concentrations in the 0.4–2 μm range are near the background levels, but concentrations in the 2–8 μm range remain elevated relative to the background, but lower than those on intersect 2. Further, for the later crossing there is an enhancement of the concentrations of droplets greater than 15 μm. The combination of these two effects is a broadening of the cloud droplet spectrum.

[11] For the east plume, the cloud response to the seeding on specific crossings was generally similar to that observed on the following crossing as shown in Figure 3 (bottom) for plume crossings 14 and 15. The large-drop enhancement relative to the background observed in these two crossings is nearly identical, although the sampling was made $\sim$3 minutes apart and laterally displaced by $\sim$3 km along the seeding line. Although the seeding effects were clearly observed in all of the east-plume crossings, the west-plume crossings (as will be shown below) did not show a similar uniform response.

[12] To further characterize the plume intersects and the background regions and to examine the east-west plume differences, we used two objective indicators—cloud effective diameter and cloud droplet spectrum width (Figures 4a and 4b). The effective diameter estimates indicate about a 2 μm increase relative to the background for the east plume intersects. The west plume crossings, however, show a more variable effective diameter with a mean close to the background values. The cloud Liquid Water Content (LWC) (not shown) is also about 10% higher in all the east plume intersects than the background values. Although the flare aerosols may experience super-saturation well below the peak super-saturation near cloud base [*Wood et al.*, 2002, Figure 4c], the largest aerosols can activate, grow by vapor deposition, and increase the liquid water content.

[13] To estimate the cloud Drop Size Distribution (DSD) width, the FSSP data were fitted to a truncated lognormal distribution using a fitting procedure described by *Feingold and Levin* [1986]. The broadening in the east plume is clearly defined in all intersects with a width that is about 0.2 μm greater than the background (in which the width, and effective diameter decrease slightly with time). In the west plume there is some broadening in the intermediate crossings (8, 9, 12, and 13). In the later east plume crossings the broadening is associated with a decrease in the total cloud droplet concentration to about 200 cm^{-3} relative to the 220 cm^{-3} observed in the background.

[14] Although the spectral width in the east plume is broadened relative to the background starting with the early crossings (e.g. crossing 2), this initial broadening is dominated by an increase in droplets in the 3–5 μm range. But later in the sampling sequence the broadening is dominated by an increase in the larger droplets as illustrated in Figures 4c and 4d where the ratios of the droplet volumes in different size ranges in the plume to those in the closest background areas are shown. In the east plume, the plume/background volume ratios for 3–5 μm droplets remains at about 2 for all the crossings, but the 20–40 μm volume ratio increases noticeably with time to $\sim$5. The west plume, however, shows minimal large-drop enhancement. Although the averaged relative Poissonian counting error for the drops in the 3–5 μm and 20–40 μm range is about 10% and 40% respectively for the east plume intersects, since the 20–40 μm volume ratio increases gradually with time, it is unlikely that the observed increase is due to chance sampling. Further, the droplet spectra from different plume crossings (e.g., crossings 14 and 15, Figure 3, bottom) show excellent coherence.

[15] The east-plume results indicate that the giant hygroscopic nuclei added by the flare burns are activated and quickly grow to sizes that can promote collision and coalescence and enhance the large-drop population as predicted by models [e.g., *Cooper et al.*, 1997]. The results provide strong evidence that giant hygroscopic nuclei produced by the flares can (under the right conditions) stimulate the processes needed for drizzle production.

[16] Further analysis will be required to explain why there are systematic differences between the east and west plumes sampled in this study. Since the response is sensitive to the vertical velocity in the areas seeded, the natural large-eddy up and down motions in the stratocumulus clouds may cause spatial variability in the cloud response to the seeding. The apparent systematic bias between the east and west plume response may be due to chance sampling of updraft regions in the east plume compared with the west plume or the possibility that there is a systematic mean difference in

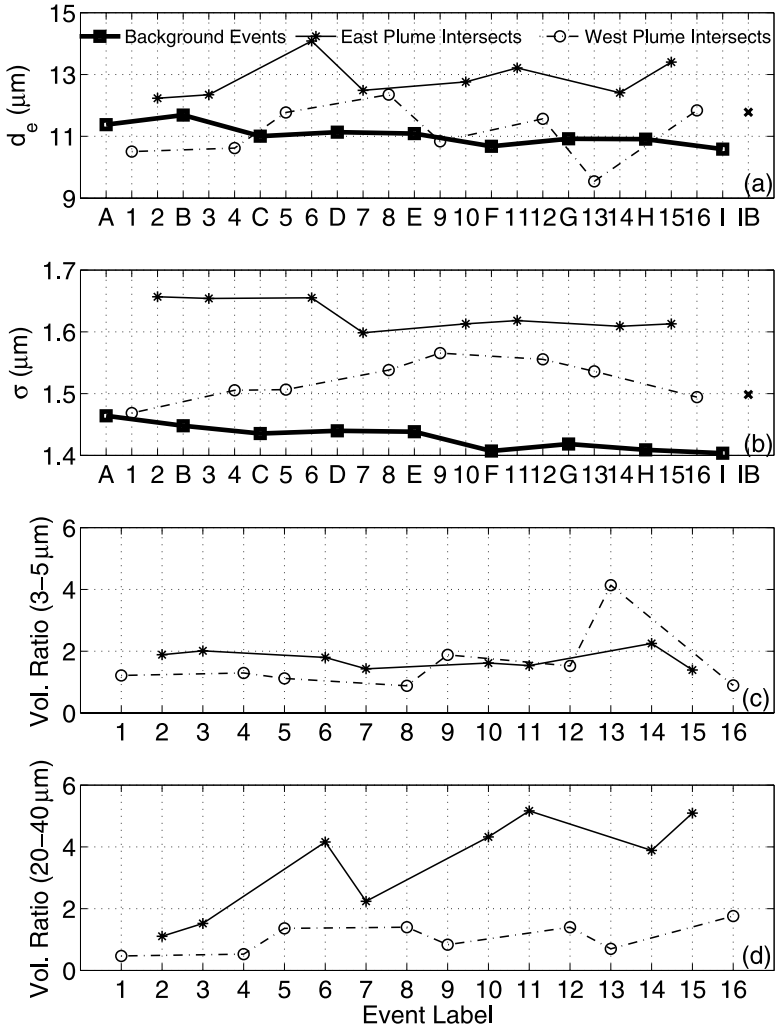

Figure 4. (a) Average effective diameter calculated using the FSSP data for all the events. (b) Cloud lognormal DSD width calculated from the fitted curve to the average FSSP data. (c) Ratio of volume of cloud droplets in the 3–5 μm range in the plumes relative to closest background values. (d) Equivalent volume ratio for droplets in the 20–40 μm range. The last value (x) in Figures 4a and 4b is the mean value of the parameters for the in-between (IB) plume intersects.

the motion fields within these two plumes. Another aspect of the seeding effects is the apparent enhancement in the PCASP aerosol concentrations in the small regions between the two plume lines starting with plume crossings 7 and 8. These effects are also seen in the cloud droplet spectra as shown by the average effective diameter and width estimates for the between plume areas shown in Figures 4a and 4b that are similar to that observed on the west plume.

5. Summary and Discussion

[17] The feasibility of artificially seeding marine stratocumulus clouds and studying the time evolution of the cloud physics due to the resulting aerosol perturbations was demonstrated. Hygroscopic seeding of a solid stratocumulus cloud layer, 200 m thick resulted in well-defined cloud droplet broadening. During the first thirty minutes following the seeding, there was a substantial increase in small cloud droplets (3–5 μm) followed by an increase in droplets greater than 15 μm, although no substantial drizzle production was detected. The cloud effective diameter increased from about 11 μm in the background to about 13 μm in the seeded plumes. About 30 minutes later, droplets in the 20–40 μm range increased by a factor of five in the plume relative to the background. Although the larger droplet production may result from condensation processes, collision and coalescence are needed to explain the increased production of large droplets.

[18] The success of this approach is made possible by the laboratory type conditions provided by marine stratocumulus clouds. These clouds have a long life-time, cover large areas, are often horizontally uniform (at least up to mesoscale), and occur in regions that are accessible by research aircraft. Because of the relative stability of these cloud fields, they offer an excellent environment to artificially modify aerosols and study the response of the clouds to such perturbations. There is, however, eddy-scale variability in these clouds that may affect the response to artificial seeding as indicated by the different responses observed in this study.

[19] The use of hygroscopic flares burned in the cloud proved to be an effective technique for making controlled

experiments. The high concentrations of cloud inactive aerosols (0.1–0.2 μm) generated by the flares and the distinctive aerosol signatures associated with two separate lines allowed the seeding plumes to be tracked in real time. The variations of the particle concentration in and around the plumes with time also provide insight into diffusion and transport properties within the clouds.

[20] The merit of the seeding approach points to the potential for future more comprehensive studies as a means of evaluating LES and cloud models [e.g., *Feingold et al.*, 1999; *Cooper et al.*, 1997; *Jiang et al.*, 2002] and studying basic microphysical processes. The use of multiple observing platforms and remote sensing systems (e.g. cloud radar), the application of different seeding agents, and carrying out experiments in a variety of configurations and cloud background conditions could support modeling and process studies leading to an improved understanding of aerosol-cloud interactions due to both natural and man-made causes.

[21] **Acknowledgment.** The research was supported by ONR grant N00014-06-0558 and NOAA grant NA17RJ1226.

References

Ackerman, A. S., O. B. Toon, D. E. Stevens, and J. A. Coakley Jr. (2003), Enhancement of cloud cover and suppression of nocturnal drizzle in stratocumulus polluted by haze, *Geophys. Res. Lett.*, *30*(7), 1381, doi:10.1029/2002GL016634.

Albrecht, B. A. (1989), Aerosols, cloud microphysics, and fractional cloudiness, *Science*, *245*, 1227–1230.

Cooper, W. A., R. T. Bruintjes, and G. K. Mather (1997), Some calculations pertaining to hygroscopic seeding with flares, *J. Appl. Meteorol.*, *36*, 1449–1469.

Durkee, P. A., K. J. Noone, and R. T. Bluth (2000), The Monterey area ship track experiment, *J. Atmos. Sci.*, *57*, 2523–2541.

Feingold, G., and Z. Levin (1986), The lognormal fit to raindrop spectra from frontal convective clouds in Israel, *J. Appl. Meteorol.*, *25*, 1346–1363.

Feingold, G., W. R. Cotton, S. M. Kreidenweis, and J. T. Davis (1999), The impact of giant cloud condensation nuclei on drizzle formation in stratocumulus: Implications for cloud radiative properties, *J. Atmos. Sci.*, *56*, 4100–4117.

Jiang, H., G. Feingold, and W. R. Cotton (2002), Simulations of aerosol-cloud-dynamical feedbacks resulting from entrainment of aerosol into the marine boundary layer during the Atlantic Stratocumulus Transition Experiment, *J. Geophys. Res.*, *107*(D24), 4813, doi:10.1029/2001JD001502.

Mather, G. K., D. E. Terblanche, F. E. Steffens, and L. Fletcher (1997), Results of South African cloud seeding experiments using hygroscopic flares, *J. Appl. Meteorol.*, *36*, 1433–1447.

Sharon, T. M., et al. (2006), Aerosol and cloud microphysical characteristics of rifts and gradients in maritime stratocumulus clouds, *J. Atmos. Sci.*, *63*, 983–997.

Stevens, B., et al. (2005), Pockets of open cells and drizzle in marine stratocumulus, *Bull. Am. Meteorol. Soc.*, *86*, 51–57.

Twomey, S. (1977), The influence of pollution on the shortwave albedo of clouds, *J. Atmos. Sci.*, *34*, 1149–1152.

Wood, R., S. Irons, and P. R. Jonas (2002), How important is the spectral ripening effect in stratiform boundary layer clouds? Studies using simple trajectory analysis, *J. Atmos. Sci.*, *59*, 2681–2693.

B. A. Albrecht and V. P. Ghate, Division of Meteorology and Physical Oceanography, Rosenstiel School of Marine and Atmospheric Science, University of Miami, 4600 Rickenbacker Causeway, Miami, FL 33149, USA. (vghate@rsmas.miami.edu)

D. W. Breed, Research Application Laboratory, National Center for Atmospheric Research, P.O. Box 3000, Boulder, CO 80307-3000, USA.

H. H. Jonsson, Center for Interdisciplinary and Remotely Piloted Aircraft Studies, 3240 Imjin Road, Hangar #510, Marina, CA 93933-5101, USA.

P. Kollias, Department of Atmospheric and Oceanic Sciences, McGill University, 805 Sherbrooke Street West, Montreal, Que., Canada H3A 2K6.